Nanostructures

DOI: 10.1002/anie.200903524

Polymer-Functionalized Platinum-On-Gold Bimetallic Nanorods**

*Bishnu P. Khanal and Eugene R. Zubarev**

Physical and chemical properties of nanosized crystals are known to be a function of their size, morphology, and chemical composition.[1–6] Hence, over the past decade many research groups have focused on controlling the shape of inorganic nanostructures,[7–12] and many low-symmetry nanocrystals have been produced.[13–20] In this respect, one-dimensional structures are particularly interesting objects whose optical and catalytic properties strongly depend on their shape anisometry.[14–17] This unique feature of metallic nanorods has already found several applications in nanotechnology[21] and biomedical research.[22,23] Moreover, four examples of bimetallic nanorods[24–27] have been described in the last few years. It is believed that bimetallic platinum-on-gold and palladium-on-gold nanostructures may open a new direction in the area of catalysis.[28–30] However, all bimetallic nanorods reported to date are only soluble in water and therefore cannot catalyze any reactions in organic solvents. In fact, there are no examples of any platinum or palladium nanostructures covalently functionalized with polymer chains, which could render them soluble in organic media. Herein we describe the first example of polymer-functionalized platinum-on-gold nanostructures. We use gold nanorods as templates and demonstrate how a polycrystalline continuous shell of platinum can be deposited on their surface and subsequently functionalized with organic molecules. In addition, we provide conclusive evidence of the functionalization of the platinum shell by direct visualization of the polymer surface layer by electron microscopy and its detection by ^{1}H NMR spectroscopy.

The seed-mediated method developed by Murphy and coworkers[1] and later modified by El-Sayed and Nikoobakht[2] produces single-crystalline gold nanorods (Au NRs). However, the conversion of Au^I ions to Au^0 in this method is only 10–15%,[31] and the majority of ions remains in solution after the growth of Au NRs is complete. Our systematic studies revealed that the amount of ascorbic acid used for the reduction of Au^I ions is critically important, and addition of 10 mol% ascorbic acid after completed nanorod growth makes their size distribution much narrower. Figure 1a shows a representative TEM image of Au NRs prepared by this modified method. The analysis of 250 nanorods shown in Figure 1a revealed that their average length and width measure 52.8 and 11.4 nm, respectively, and the standard deviation (SD) for both dimensions is less than 9%. These results represents a significant improvement in comparison with Au nanorods prepared under the standard conditions (SD ≈ 20%).[1,2]

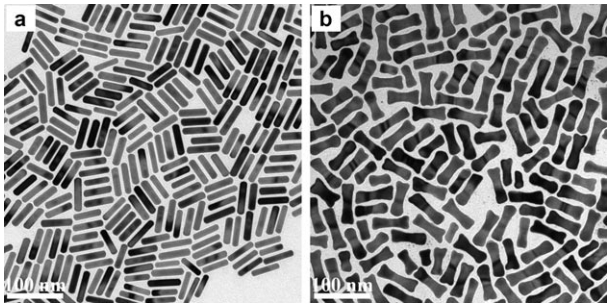

Figure 1. TEM images of a) CTAB-stabilized Au NRs and b) Au dogbones. CTAB = cetyltrimethylammonium bromide.

Further introduction of ascorbic acid allows conversion of Au^I ions remaining in the growth solution into metallic gold and its deposition onto the surface of Au NRs.[32] However, this rapid addition of ascorbic acid results in a nonuniform deposition of gold, and the shape of the nanorods changes to a so-called dogbone (Figure 1b). It has been suggested[32] that the preferential deposition on the tips of the nanorods is due to a denser packing of CTAB molecules on the side facets, which have a much lower curvature. Upon the conversion of nanorods to dogbones, the length increases from 53 to 63 nm, whereas the average width changes from 11.4 to 18.5 nm. This transformation corresponds to a decrease in the aspect ratio of the nanorods from 4.6 to 3.4 and an almost twofold increase in their mass.

After the gold ions were reduced (ca. 2 h), we added excess ascorbic acid and subsequently 25 mol% Pt^{IV} ions. Under these conditions, a slow reduction of platinum takes place at 30 °C within 12 h. The color of the dogbones solution gradually changes from deep red to dark gray. A TEM analysis revealed that the deposition of platinum proceeds mainly on the tips of the dogbones and converts them into more symmetrical dumbbell-shaped structures (Figure 2a). These bimetallic objects measure on average 67 × 23 nm (SD ≈ 15%) and have a polycrystalline structure composed of multiple particles of Pt, which are oriented randomly and fused together near the tips of the gold core. This behavior is in contrast to single-crystalline bimetallic Au/Pt nanorods prepared by reduction of Pt^{II} ions.[26a]

The deposition of platinum can be resumed and repeated several times if a new portion of Pt^{IV} ions is introduced. This procedure allows us to increase the coverage of dumbbells and produce more uniform Au/Pt nanorods with a nearly rectangular shape. Figure 2b shows the structures obtained

[*] B. P. Khanal, Prof. E. R. Zubarev
Department of Chemistry, Rice University
Houston, TX 77005 (USA)
Fax: (+1) 713-348-5155
E-mail: zubarev@rice.edu
Homepage: http://www.owlnet.rice.edu/~zubarev/

[**] This work was supported by the NSF CAREER Award (DMR-0547399), Robert A. Welch Foundation (C-1703), and Alfred Sloan Foundation.

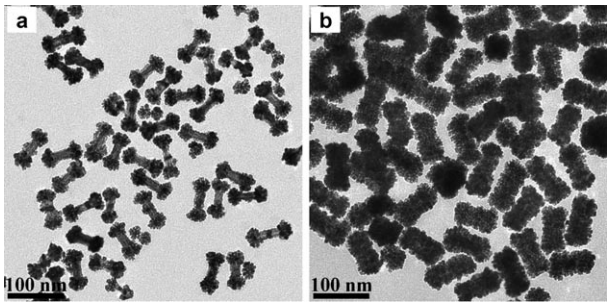

Figure 2. TEM images of a) bimetallic Au/Pt dumbbells and b) rectangular Au/Pt nanorods. Samples prepared by drop-casting of aqueous solutions.

after the addition of 50 mol% Pt^{IV} ions to a solution of the dumbbells depicted in Figure 2a. The resulting nanorods are polycrystalline and contain numerous particles of platinum residing on the inner gold core, which is visible in many nanostructures. The average size of these Au/Pt nanorods is 82×38 nm (SD $\approx 12\%$), and their aspect ratio drops to 2.2. The energy-dispersive X-ray spectroscopy (EDS) elemental analysis revealed that the content of platinum in these bimetallic nanorods is about 60%. It is interesting to note that the deposition of platinum stops after the full coverage of the gold core is complete. Therefore, our attempts to increase the size of Au/Pt nanorods by adding Pt^{IV} ions in the presence of excess ascorbic acid were unsuccessful. This finding suggests that under these conditions the reduction of platinum ions proceeds only on the surface of metallic gold.

The morphological and compositional transformations of structures shown in Figures 1 and 2 are accompanied by specific changes in their optical properties (Figure 3). The

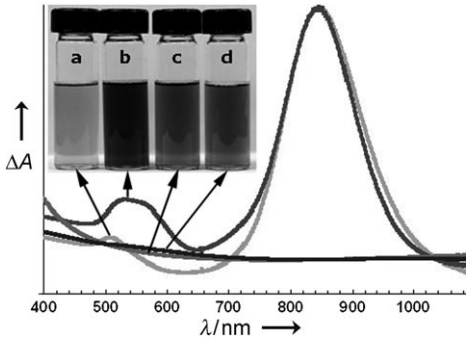

Figure 3. Normalized UV/Vis absorption spectra collected from the aqueous solutions of a) Au NRs, b) Au dogbones, c) bimetallic Au/Pt dumbbells, and d) rectangular Au/Pt nanorods.

initial Au NRs exhibit two plasmon resonance peaks at 510 (transverse) and 842 nm (longitudinal). The color of the aqueous solution of pure Au NRs is brown, which changes to dark brown/red when ascorbic acid reduces the remaining Au^{I} ions (Figure 3 inset). The color intensifies during the conversion of Au NRs to dogbones because the concentration of metallic gold increases by a significant factor. Remarkably, the position and the width of the longitudinal plasmon of dogbones remains virtually the same as that of the initial Au NRs (Figure 3). This finding is very surprising given the fact that the aspect ratio decreases from 4.6 to 3.4 during this process. The longitudinal plasmon is known to be highly sensitive to the aspect ratio of 1D nanostructures, but it also depends on the overall shape, symmetry, and the total mass of nanorods. The changes and the interplay of these parameters appear to offset the expected blue shift of the longitudinal peak. Upon the addition of platinum ions, the color changes from brown/red to gray within several hours. After the first deposition of Pt is complete (dumbbells), the plasmon peaks disappear completely. The subsequent conversion of dumbbells into rectangular Au/Pt nanorods does not bring any changes (Figure 3). The absence of the UV absorption confirms the complete encapsulation of the gold core and the formation of core–shell platinum-on-gold nanostructures.

To functionalize the resulting platinum-on-gold nanostructures, we attempted to replace CTAB with a functionalized thiol (mercaptophenol). While this strategy has been successful for pure gold nanorods,[33,34] it has never been applied to any other metals, including platinum, which form a much weaker bond with sulfur. When a concentrated 1.2 M solution of mercaptophenol in THF is introduced dropwise into an aqueous solution of CTAB-stabilized platinum-on-gold nanorods, the mixture remains homogeneous for several hours, whereas the intensity of its color gradually decreases. After 10–12 h a fine black powder forms in solution and slowly precipitates. The supernatant is then decanted and the precipitate is washed multiple times with THF/water mixture. The observed gradual loss of the water solubility suggests that the CTAB bilayer stabilizing the Pt shell has been replaced with mercaptophenol.

When a dichloromethane solution of carboxy-terminated polystyrene (PS-COOH, MW = 5000 g mol^{-1}) is added to the isolated nanorods functionalized with mercaptophenol, no dissolution takes place. However, addition of esterification agents (diisopropyl carbodiimide (DIPC) and 4-(*N*,*N*-dimethylamino)pyridinium-4-toluenesulfonate (DPTS)) results in complete dissolution of nanorods within 10–15 min. Interestingly, the coupling reaction can be monitored by regular TLC, as the new product moves on the silica gel in a 10% MeOH/CH_2Cl_2 mixture ($R_f = 0.5$). After further 4 h, the product is purified by centrifugal ultrafiltration. The removal of free polystyrene is confirmed by TLC and size exclusion chromatography (SEC). The isolated product is highly soluble in many organic solvents, including dichloromethane, chloroform, acetone, and THF. Most importantly, the high solubility of the resulting nanorods allows for their characterization by ^{1}H NMR spectroscopy (not shown), which reveals all the characteristic signals of polystyrene. Because no appreciable amount of free polystyrene is detected in the isolated product by SEC, we conclude that the resonances observed in the NMR spectrum are generated by PS chains covalently attached to mercaptophenol ligands covering the platinum shell of nanorods. This finding also serves as indirect evidence that the replacement of CTAB by mercaptophenol on the surface of the platinum shell was successful.

Remarkably, the polystyrene shell on the surface of Au/Pt nanorods can be directly visualized by TEM. Figure 4a,b

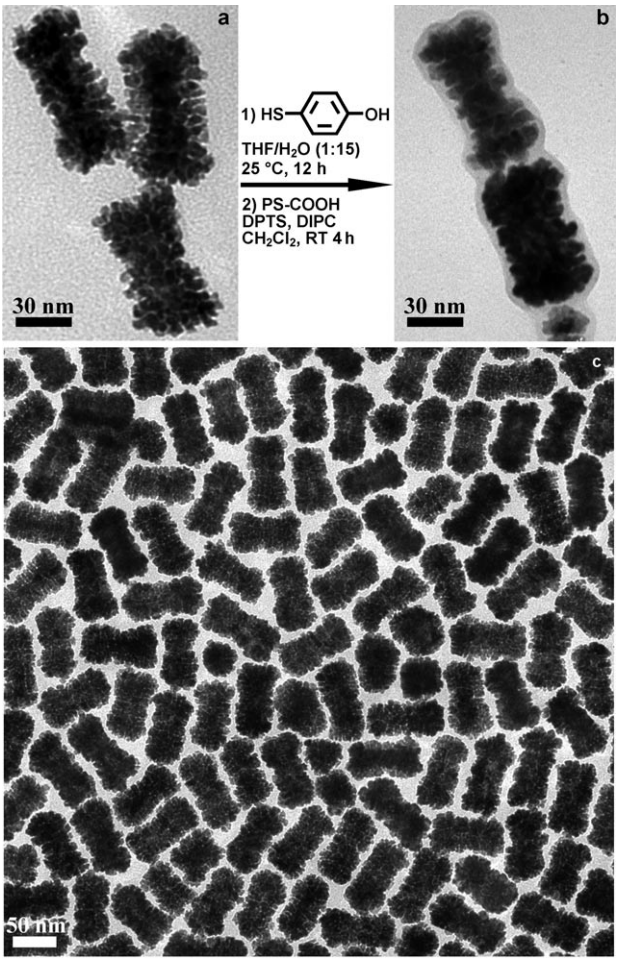

Figure 4. TEM images of Au/Pt nanorods a) before and b,c) after functionalization with polystyrene chains which are covalently attached to mercaptophenol monolayer on the platinum shell.

shows high-magnification images of nanorods before and after the functionalization. The CTAB-stabilized nanorods do not exhibit any organic layer on their surface, which is due to the small size of the surfactant molecules. In contrast, the nanorods isolated after the esterification reaction display a uniform continuous layer measuring 4–5 nm in thickness. The organic shell precisely follows the contour and the roughness of the bimetallic nanostructures. To our knowledge this is the first direct visualization of a polymer shell covalently attached to inorganic rod-like nanostructures. It also reveals that the initial replacement of CTAB by mercaptophenol proceeds uniformly and is not limited to the tip areas. Interestingly, the organic shell can only be visualized when the nanorods are almost completely isolated. The presence of closely positioned neighboring nanorods eliminates the fine contrast between the PS shell and the amorphous carbon substrate. Figure 4c shows a low-magnification image of densely packed Au/Pt/PS nanorods. In this case, the gaps between the structures are occupied by PS chains, which completely cover the carbon grid substrate and therefore can no longer be distinguished from it. Nevertheless, the average interrod distance is similar to the thickness of the PS shell (4–5 nm). Moreover, the attachment of polystyrene is confirmed by a 20% mass increase of nanorods isolated after the esterification reaction. This mass gain enables a rough estimation of the average number of polymer chains (MW = 5000 Da) attached to each nanorod (MW $\approx 8\times10^8$ Da), which translates into approximately 32000 chains for a 20% mass increase. The surface area of 28×82 nm Au/Pt nanorods is at least 64300 nm^2, hence the grafting density of the polystyrene is $64300/32000 = 2.01$ chains nm^{-2}. This value is in good agreement with the previously reported values for PS-functionalized Au NRs.[33] At the same time, it is nearly 22 times higher than that reported for PEO-functionalized nanoshells prepared by direct replacement of small ligands with thiol-terminated polymer chains of the same molecular weight (5000 Da).[35]

In conclusion, we have demonstrated how the morphology and the chemical composition of platinum-on-gold nanocrystals can be controlled and how their conversion into hybrid organic–inorganic structures can be achieved. The two-step covalent functionalization of the platinum shell described herein offers a unique possibility to prepare soluble Pt nanostructures capable of catalyzing reactions in organic media, which will be described in due course.

Experimental Section

Synthesis of nanorods: Single-crystalline gold nanorods were prepared on a 500 mL scale using a modified seed-mediated method described elsewhere.[33] To convert Au NRs into dogbones, aqueous ascorbic acid (0.1 M, 5 mL) was added to Au NRs (500 mL). The color changed from brown to dark brown/red within 10 min, and the reaction mixture was kept undisturbed for 2 h. After the formation of dogbone-shaped nanorods, additional ascorbic acid (solid, 1 g) was added and the content of the flask was stirred until the solution became clear. Then, $H_2PtCl_6{\cdot}6H_2O$ in water (1.974×10^{-3} M, 50 mL) and subsequently HCl(aq) (0.2 M, 2 mL) were added to the reaction flask. The reaction mixture was left undisturbed for 12 h at 30°C. Addition of further Pt^{IV} (1.974×10^{-3} M, 100 mL) and HCl(aq) (0.2 M, 2 mL) was carried out to convert dumbbells into bimetallic rectangular Au/Pt nanorods.

Functionalization with thiol: A concentrated THF solution of 4-mercaptophenol (5 g in 30 mL) was added dropwise to the growth solution of Au/Pt nanorods under vigorous stirring. This addition caused a change in color (from dark brown to black), and the mixture was allowed to stir at 27°C for 12 h. The black precipitate was collected after centrifugation (3750 rmp, 10 min). Residual CTAB and 4-mercaptophenol were removed by repeated rinsing with THF and water. The total weight of the dried product was typically 100 mg.

Attachment of polystyrene: Dichloromethane (2 mL) was added to mercaptophenol-functionalized Au/Pt nanorods (100 mg), and the mixture was stirred for several minutes before the addition of carboxy-terminated polystyrene (5 kDa, 100 mg). DPTS (15 mg) was added next, and the mixture was allowed to stir for 5 min before DIPC was introduced dropwise (15 drops). The product was isolated after 3–4 h using centrifugal ultrafiltration (molecular weight cutoff (MWCO) = 30 kDa). This procedure afforded the final product (120 mg), which was characterized by UV/Vis and ^{1}H NMR spectroscopy (300 MHz, CD_2Cl_2): $\delta = 2.3$–1.3 (br, 150 H), 7.4–6.3 ppm (br, 250 H).

Received: June 30, 2009
Published online: August 13, 2009

Keywords: functionalization · gold · nanostructures · organic–inorganic hybrid composites · platinum

[1] N. R. Jana, L. Gearheart, C. J. Murphy, *Adv. Mater.* **2001**, *13*, 1389.
[2] B. Nikoobakht, M. A. El-Sayed, *Chem. Mater.* **2003**, *15*, 1957.
[3] R. C. Jin, C. A. Mirkin, K. L. Kelly, G. C. Schatz, J. G. Zheng, *Science* **2001**, *294*, 1901.
[4] I. Pastoriza-Santos, L. M. Liz-Marzan, *Nano Lett.* **2002**, *2*, 903.
[5] Y. G. Sun, Y. N. Xia, *Science* **2002**, *298*, 2176.
[6] S. E. Habas, H.-J. Lee, V. Radmilovic, G. A. Somorjai, P. Yang, *Nat. Mater.* **2007**, *6*, 692.
[7] a) P. Mulvaney, *Langmuir* **1996**, *12*, 788; b) J. Perez-Juste, I. Pastoriza-Santos, L. M. Liz-Marzan, P. Mulvaney, *Coord. Chem. Rev.* **2005**, *249*, 1870; c) S. W. Prescott, P. Mulvaney, *J. Appl. Phys.* **2006**, *99*, 123504; d) M. Das, N. Sanson, D. Fava, E. Kumacheva, *Langmuir* **2007**, *23*, 196.
[8] Z. Y. Tang, Z. L. Zhang, Y. Wang, S. C. Glotzer, N. A. Kotov, *Science* **2006**, *314*, 274.
[9] Q. L. Zhang, S. Gupta, T. Emrick, T. P. Russell, *J. Am. Chem. Soc.* **2006**, *128*, 3898.
[10] B. D. Korth, P. Keng, S. E. Bowles, T. Kowalewski, K. W. Nebesny, J. Pyun, *J. Am. Chem. Soc.* **2006**, *128*, 6562.
[11] B. Liu, H. C. Zeng, *J. Am. Chem. Soc.* **2005**, *127*, 18262.
[12] Q. Dai, J. G. Worden, J. Trullinger, Q. Huo, *J. Am. Chem. Soc.* **2005**, *127*, 8008.
[13] Z. W. Pan, Z. R. Dai, Z. L. Wang, *Science* **2001**, *291*, 1947.
[14] Y. Y. Yu, S. S. Chang, C. L. Lee, C. R. C. Wang, *J. Phys. Chem. B* **1997**, *101*, 6661.
[15] S. Link, M. A. El-Sayed, *J. Phys. Chem. B* **1999**, *103*, 8410.
[16] N. R. Jana, L. Gearheart, C. J. Murphy, *J. Phys. Chem. B* **2001**, *105*, 4065.
[17] Z. H. Nie, D. Fava, E. Kumacheva, S. Zou, G. C. Walker, M. Rubinstein, *Nat. Mater.* **2007**, *6*, 609.
[18] C. S. Yang, D. D. Awschalom, G. D. Stucky, *Chem. Mater.* **2001**, *13*, 594.
[19] A. T. Kelly, I. Rusakova, T. Ould-Ely, C. Hofmann, A. Luttge, K. H. Whitmire, *Nano Lett.* **2007**, *7*, 2920.
[20] S. Asokan, K. M. Krueger, V. L. Colvin, M. S. Wong, *Small* **2007**, *3*, 1164.
[21] V. M. Shalaev, W. Cai, U. K. Chettiar, H.-K. Yuan, A. K. Sarychev, V. P. Drachev, A. V. Kildishev, *Opt. Lett.* **2005**, *30*, 3356.
[22] H. Wang, T. B. Huff, D. A. Zweifel, W. He, P. S. Low, A. Wei, J.-X. Cheng, *Proc. Natl. Acad. Sci. USA* **2005**, *102*, 15752.
[23] X. H. Huang, I. H. El-Sayed, W. Qian, M. A. El-Sayed, *J. Am. Chem. Soc.* **2006**, *128*, 2115.
[24] a) C. S. Ah, S. D. Hong, D.-J. Jang, *J. Phys. Chem. B* **2001**, *105*, 7871; b) M. Z. Liu, P. Guyot-Sionnest, *J. Phys. Chem. B* **2004**, *108*, 5882; c) J. H. Song, F. Kim, D. Kim, P. Yang, *Chem. Eur. J.* **2005**, *11*, 910.
[25] Y. J. Xiang, X. C. Wu, D. F. Liu, X. Y. Jiang, W. G. Chu, Z. Y. Li, Y. Ma, W. Y. Zhou, S. S. Xie, *Nano Lett.* **2006**, *6*, 2290.
[26] a) M. Grzelczak, J. Perez-Juste, L. M. Liz-Marzan, *J. Mater. Chem.* **2006**, *16*, 3946; b) S. J. Guo, L. Wang, Y. Wang, Y. X. Fang, E. K. Wang, *J. Colloid Interface Sci.* **2007**, *315*, 363.
[27] M. Grzelczak, B. Rodriguez-Gonzalez, J. Perez-Juste, L. M. Liz-Marzan, *Adv. Mater.* **2007**, *19*, 2262.
[28] D. I. Enache, J. K. Edwards, P. Landon, B. Solsona-Espriu, A. F. Carley, A. A. Herzing, M. Watanabe, C. J. Kiely, D. W. Knight, G. J. Hutchings, *Science* **2006**, *311*, 362.
[29] M. O. Nutt, K. N. Heck, P. Alvarez, M. S. Wong, *Appl. Catal. B* **2006**, *69*, 115.
[30] N. Dimitratos, F. Porta, L. Prati, A. Villa, *Catal. Lett.* **2005**, *99*, 181.
[31] C. J. Orendorff, C. J. Murphy, *J. Phys. Chem. B* **2006**, *110*, 3990.
[32] L. Gou, C. J. Murphy, *Chem. Mater.* **2005**, *17*, 3668.
[33] B. P. Khanal, E. R. Zubarev, *Angew. Chem.* **2007**, *119*, 2245; *Angew. Chem. Int. Ed.* **2007**, *46*, 2195.
[34] a) B. P. Khanal, E. R. Zubarev, *J. Am. Chem. Soc.* **2008**, *130*, 12634; b) W.-S. Chang, L. S. Slaughter, B. P. Khanal, P. Manna, E. R. Zubarev, S. Link, *Nano Lett.* **2009**, *9*, 1152.
[35] C. S. Levin, S. W. Bishnoi, N. K. Grady, N. J. Halas, *Anal. Chem.* **2006**, *78*, 3277.

